Ordered and disordered solvates of C_{60} and $CBrCl_2H$

Jin Ye[a], Maria Barrio [a], René Céolin[a,b], Navid Qureshi[c], Philippe Negrier[d], Ivo B. Rietveld[e,f], Josep Lluís Tamarit[a,*]

Received 00th January 20xx,
Accepted 00th January 20xx

DOI: 10.1039/x0xx00000x

www.rsc.org/

The formation of co-crystals is often unexpected; however, the Buckminster fullerene, for which many solvates are known, is an excellent system to study this tendency. In the present paper, C_{60} and $CBrCl_2H$ co-crystals have been studied. Hexagonal *P6/mmm* $C_{60}\cdot 2CBrCl_2H$ co-crystals transform at 373 K to monoclinic *C2/c* $C_{60}\cdot CBrCl_2H$ co-crystals. While orientational disorder typical for C_{60} is found in the hexagonal co-crystals (as found in many C_{60} halomethane solvates), in the monoclinic co-crystals, C_{60} appears to be orientationally ordered. As for the solvent $CBrCl_2H$, two types of occupational disorder involving the distribution of the halogen atoms can be observed, comparable to the behaviour in the two polymorphs of pure $CBrCl_2H$. Within the monoclinic solvate, two sites are equally occupied by Br and Cl atoms (1/2:1/2), while one site is fully occupied by a Cl atom which leads to an average C_s symmetry for the solvent molecule. Whereas within the hexagonal co-crystals, each halogen position is occupied by 1/3:2/3 of Br or Cl atoms, respectively, leading to an average C_{3v} molecular symmetry. The anisotropy of the intermolecular interactions coincides with the symmetry of the solvate structures and can be generalized for the $C_{60}\cdot$ halomethane co-crystals.

Introduction

The spherical shape of the C_{60} fullerene molecule and its conjugated π-electron system makes it one of the best candidates for creating intricate molecular structures with high potential for applications. Despite the insulating character of the C_{60} molecule, conducting and even superconducting materials have been obtained upon intercalation with alkali atoms, which can transfer their valence electrons to the conduction bands of the C_{60} sublattice[1]. The high molecular symmetry of C_{60} gives rise to a plastic crystal at room temperature in which C_{60} is orientationally disordered due to the isotropic intermolecular potential. This characteristic causes C_{60} to be susceptible to the formation of co-crystals with other molecules, which in the case of liquid coformers are also called solvates.

It has been shown that small molecules, such as methane, can be incorporated into the octahedral voids of the C_{60} structure, but also larger molecules such as n-alcanes[2-4], halobenzenes[5,6] and even larger molecules[7-9]. Despite the variety in coforming molecules, C_{60}-C_{60} interactions still control the overall packing in these co-crystals[2,10]. The dynamics in these systems also reflects the behaviour of pure C_{60} crystals, as demonstrated by the existence of order-disorder transitions as a function of temperature[9,11-13].

It is obvious that if steric conditions are favourable, guest molecules can be substituted for others in the high-symmetry lattice of fcc C_{60}. If in such a case, the new guest molecule does not display the required symmetry elements for the lattice site concerned, the symmetry of the molecule must be "generated" by orientational disorder or by occupational disorder (14; 15; 16). Quite a number of solvates containing C_{60} and a halomethane $CX_{4-n-m}Y_nH_m$ (n,m = 0, ..., 4, n+m≤4) has been studied up to now[3, 4, 12; 17-27]). The overall packing of the crystal structures of this type of co-crystals has been related to the apparent symmetries of the halomethane compounds as well as to the asymmetry in the intermolecular interactions that are mainly van der Waals. Despite the weak interactions, a wide range of lattice symmetries has been found, which happen to be independent of the molecular symmetry of the guest molecule. For example, for halomethane molecules with C_{2s} symmetry, such as CBr_2Cl_2, $CBr_2(CH_3)_2$ and CBr_2H_2, the solvates with the first two molecules display a hexagonal structure with orientational disorder for both C_{60} and solvent molecules[24]; however, for the third molecule, C_{60} and solvent molecules are orientationally ordered in the solvate structure (monoclinic *C2/m*) in spite of the overall hexagonal packing[25]. It appears to be a consequence of stronger host-guest intermolecular interactions when compared to the preceding cases. Similar results were found for the solvate $C_{60}\cdot 2CBrClH_2$ (monoclinic *C2/m*), both molecules possessing orientational order, although the two halogens, Br and Cl, were distributed over two sites with equal occupational factors[12]. Moreover, C_{60} solvates have been reported in which a phase

[a.] *Departament de Física, ETSEIB, Universitat Politècnica de Catalunya, Diagonal 647, 08028 Barcelona, Catalonia, Spain.*

[b.] *LETIAM, EA7357, IUT Orsay, Université Paris Sud, rue Noetzlin, 91405 Orsay Cedex, France.*

[c.] *Institut Laue Langevin, 71 avenue des Martyrs - CS 20156 - 38042 GRENOBLE CEDEX 9, France.*

[d.] *LOMA, UMR 5798, CNRS, Université de Bordeaux, F-33400 Talence, France.*

[e.] *Normandie Université, Laboratoire SMS, EA 3233, Université de Rouen, F76821 Mont Saint Aignan, France.*

[f.] *Université Paris Descartes, Faculté de Pharmacie, 4 avenue de l'observatoire, 75006 Paris, France.*

E-mail: josep.lluis.tamarit@upc.edu Tel: +34934016564

†Electronic Supplementary Information (ESI) available: [details of any supplementary information available should be included here]. See DOI: 10.1039/x0xx00000x

`

transition changes the orientationally disordered room-temperature structure to a low-temperature crystal with well-defined orientational order for C_{60}[11,13,28-30]. In these crystal structures, strong intermolecular interactions are thought to cause orientational order for C_{60} molecules and in some cases for the solvent guest molecules.

Nevertheless, how the symmetry of the guest molecules influences the interactions and the phase behaviour of the C_{60} co-crystals is still a matter of debate. In this work, we report on co-crystals containing C_{60} and $CBrCl_2H$. Similar co-crystals between C_{60} and CBr_3H or CCl_3H with C_{3v} symmetry have been studied before and phase transitions from a high-temperature hexagonal (orientational disordered) phase to a triclinic (orientationally ordered) low-temperature phase have been reported[31]. Halomethane CXY_2H (X,Y=Br,Cl) compounds with C_s molecular symmetry are known to simulate the C_{3v} symmetry (site occupational disorder between Br and Cl atoms with occupational factors of 1/3 and 2/3, respectively) or to keep the C_s symmetry, while two halogen atoms share two sites (occupational factors of ½ and ½ for Br and Cl) and the third one remains at one well-defined crystallographic site[32]. In the present paper, two solvates will be discussed, one exhibiting a hexagonal lattice symmetry the other displaying a monoclinic lattice structure both reflecting the behaviour described above. A simple correlation between the volumes of the asymmetric unit of the crystals and the molecular volume of the solvent molecules will demonstrate the role of the molecular symmetry on the symmetry and packing of the C_{60} solvates with halomethane compounds.

Experimental

Fullerene C_{60} was purchased from TermUSA with a purity higher than 99.98%. Bromodichloromethane ($CBrCl_2H$) with a purity higher than 98% was obtained from Aldrich.

C_{60} crystals and solvent $CBrCl_2H$ were mixed in screw-cap tubes at room temperature. The fcc C_{60} crystals took several days to transform into the hexagonal solvate.

The structural properties of the co-crystals containing C_{60} and $CBrCl_2H$ were studied by X-ray powder diffraction (XRPD) using a high-resolution vertically mounted INEL cylindrical position-sensitive detector (CPS-120, angular step 0.029°-2θ over a 2θ-range from 2 to 115°) and a Debye-Scherrer geometry equipped with a monochromatic Cu $K\alpha_1$ (λ =1.5406 Å) radiation working at 35 kV and 35 mA. The system was equipped with a liquid nitrogen 700 series Cryostream Cooler (Oxford Cryosystems) with an accuracy of 0.1 K. Samples were placed into 0.5-mm-diameter Lindemann capillaries, which were rotating around their axes during data collection to reduce the effects of preferential orientation.

The peak positions were determined after pseudo-Voigt fitting of the Bragg peaks. Lattice parameters were determined using DICVOL06. Rietveld refinement was carried out with the Materials Studio package[33] for the orientationally ordered C_{60} molecule, whereas the FullProf Suite[34] was used to describe the orientationally disordered C_{60} molecule with spherical harmonics. The $CBrCl_2H$ molecule was modelled in both cases as a rigid body (C-Cl: 1.757 Å, C-Br: 1.9296 Å, C-H: 1.09 Å).

Differential scanning calorimetry (DSC) and thermogravimetry (TG) analyses were conducted with a Q100 and a TA Q50 from TA Instruments, respectively. Sample masses ranged between 5 and 15 mg and heating and cooling rates of 2 K min^{-1} were used. When required, DSC measurements were performed in hermetically sealed high-pressure stainless steel pans from Perkin-Elmer to resist the vapor pressures of the solvent.

The morphology of the crystals was examined with a JEOL-7100F scanning electron microscope (SEM) with a scanning voltage of 20 kV.

Results and discussion

Two days after mixing fcc C_{60} crystals and liquid $CBrCl_2H$, the solution turned grey in colour. Crystals extracted from the mother liquor and observed immediately by scanning electron microscopy were hexagonally shaped as can be seen in Fig. 1.

The hexagonally shaped crystals were investigated by TG to determine the C_{60}:solvent stoichiometry. The mass of the selected crystals in a small quantity of mother liquor was recorded at room temperature as a function of time until it had stabilized, indicating that all the mother liquor had evaporated. Immediately afterwards, the remaining sample was heated up to 673 K (solid black circles in Fig. 2). Using the same procedure, the crystals were also analysed by DSC (black line in Fig. 2). Both TG and DSC profiles indicate that complete desolvation involves a mass loss of ca. 30% and corresponds to a $C_{60}{\cdot}2CBrCl_2H$ solvate; however, it can be seen that the desolvation process consists of two steps (see the deconvolution of the DSC curve in Fig. 2 as well as the inflection point in the TG curve). In order to understand the convoluted process, DSC measurements were carried out with the crystals in the mother liquor in high-pressure sealed pans (Fig. 3). The DSC signal (Fig. 3a) demonstrates: (i) the existence of an endothermic peak P1 corresponding to the melting of $CBrCl_2H$ solid in excess, which is found to be within error at the same temperature as the melting point of the pure solvent and translates into a degenerate eutectic equilibrium in the phase diagram (Fig. 3b); (ii) a peak P2 at around 373 K corresponding to a peritectic solid-solid transition in which the hexagonal solvate transforms into a different structure with a change in the stoichiometry (see below); (iii) finally, a peak P3 at ca. 430 K reflecting the desolvation process of the solvate obtained at 373 K. A schematic phase diagram is presented in Fig. 3b.

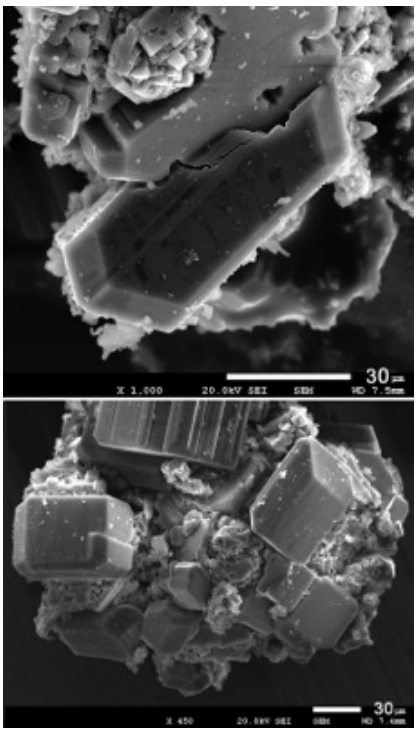

Fig.1. Scanning electron microscopy (JEOL-7100F, scanning voltage of 20 kV) photographs of hexagonal C_{60}·2$CBrCl_2H$ crystals. The white horizontal bars correspond to a length of 30 µm.

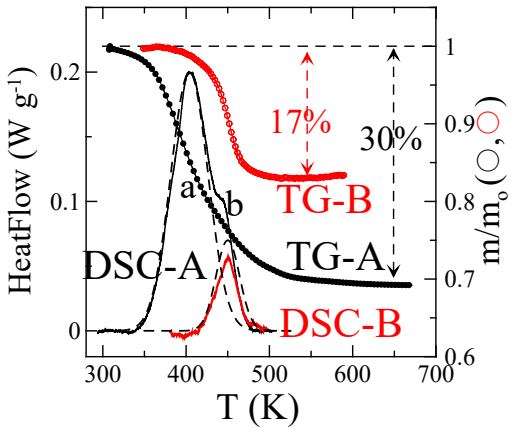

Fig. 2. Thermogravimetric (right-hand axis) and calorimetric (left-hand axis) data obtained in pierced aluminum pans **(A-black)** of the hexagonal C_{60}·2$CBrCl_2H$ solvate crystals: TG curve (solid circles) and DSC curve (solid line) and **(B-red)** of the monoclinic C_{60}·$CBrCl_2H$ solvate crystals: TG curve (open circles) and DSC curve (solid line). Dashed black DSC curves represent the deconvolution of the DSC-A into two contributions (see text).

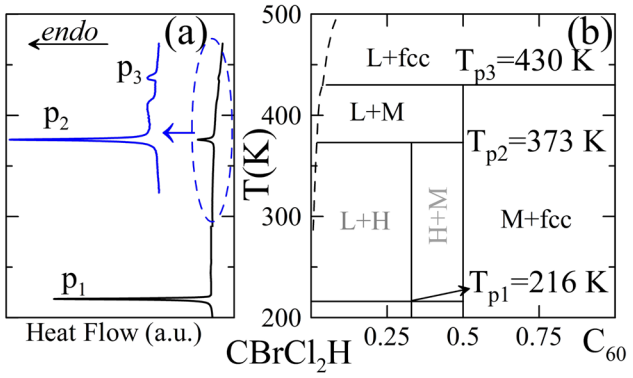

Fig. 3. (a) DSC signal of the hexagonal C_{60}·2$CBrCl_2H$ crystals in an excess of mother liquor in a sealed pan. (b) Schematic phase diagram with the eutectic (Tp_1) and peritectic (Tp_2) invariant equilibria involving the hexagonal (H) C_{60}·2$CBrCl_2H$ solvate and the peritectic Tp_3 involving the monoclinic (M) C_{60}·$CBrCl_2H$ solvate. The liquidus curves are provided as guides for the eyes.

The hexagonally shaped crystals together with an excess of mother liquor were placed into a Lindemann capillary, which was subsequently sealed. An X-ray diffraction pattern was obtained at room temperature and indexed using DICVOL06 resulting in a hexagonal unit cell (Fig. 4). The systematic absences pointed to the P6/mmm space group, which is the most common structure of co-crystals containing C_{60} and halomethane derivatives[18,19,23,35,36]. Its structure was solved using the procedure previously described for the C_{60}·2$CBrClH_2$ solvate[12]. In short, the structure was evaluated using the FullProf suite[34], while the C_{60} molecule was described with spherical harmonics as a homogeneous distribution of 60 C-atoms positioned on a sphere with a radius of 3.59 Å and located at the 1a Wyckoff positions. Rigid $CBrCl_2H$ molecules were placed at the prismatic hexagonal voids, the (1/3, 1/3, 1/2) positions, while the positions of the halogen atoms exhibit a disorder with each site occupied for 2/3 with a Cl atom and for 1/3 with a Br atom. Such occupational disorder coincides with one of the proposed models ("mode 2") for the monoclinic structure of the pure solvent[32]. The final Rietveld refinement yielded R_{wp}= 3.72% and R_p=5.07 % (see Supplementary Information for details). The refined lattice parameters were found to be a = 10.131(2) Å, c = 10.135(2) Å and V_{cell} = 900.9(2) Å^3, while the final refined position of the central carbon atom of the disordered solvent molecule was found to be (0.349(4), 0.719(3), 0.483(6)), i.e. very close to the prismatic hexagonal voids. Fig. 4 provides the experimental and refined X-ray patterns for the hexagonal C_{60}·2$CBrClH_2$ solvate. Additional X-ray diffraction experiments in an open capillary have demonstrated that this solvate is not stable in air at room temperature (see Fig. S1 in the Supplementary Information).

`

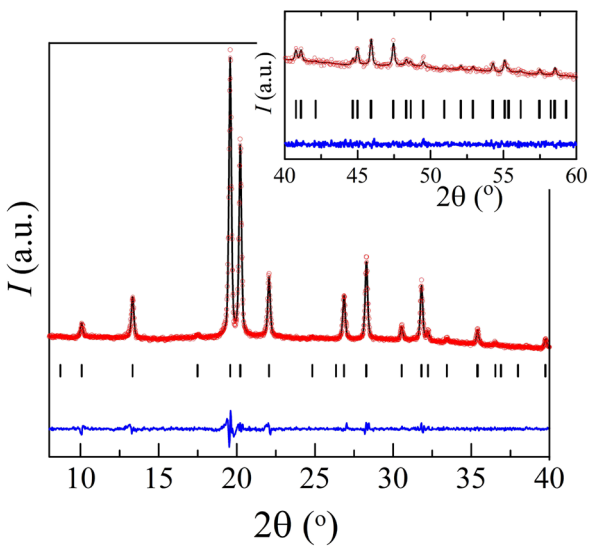

Fig. 4. Experimental (red circles) and calculated (black line) X-ray powder diffraction pattern of hexagonal C_{60}·2$CBrCl_2H$ at room temperature along with the difference profile (blue line) and Bragg reflections (vertical bars). The inset provides the data between 40 and 60° (2θ) at an increased scale.

In order to characterize the phase obtained in the DSC experiments at ca. 373 K, which resulted in the two-steps desolvation process (Fig. 2), X-ray diffraction measurements were carried out on the hexagonal co-crystals as a function of temperature in a sealed capillary. Fig. 5 contains several patterns between room temperature and 455 K above the peritectic desolvation phenomena (see also Fig. 3). Because the pattern at 373 K indicates the appearance of a different structure, more crystals were prepared by separately heating up hexagonal co-crystals to 373 K. The resulting powder was placed in a Lindemann capillary for a high signal/noise ratio X-ray powder diffraction measurement at room temperature. Results are shown in Fig. 6. Crystals of the new structure were analysed by TG and DSC (see Fig. 2). TG results (curve TG-B in Fig, 2) indicate a mass loss of 17%, which corresponds to a solvate with a stoichiometry of 1:1 (C_{60}·$CBrClH_2$ solvate). Moreover, DSC measurements in open pans revealed a single peak (curve DSC-B in Fig. 2), which can be ascribed to the desolvation of the 1:1 solvate. Thus, the convoluted peak for the hexagonal-shaped co-crystals can be deconvoluted into a two-step desolvation process of C_{60}·2$CBrCl_2H$ transforming into C_{60}·$CBrCl_2H$, which subsequently loses its solvent entirely resulting in a liquid and fcc C_{60} with defects and stacking faults[37].

For the structure of C_{60}·$CBrClH_2$, patterns were indexed with DICVOL06 leading to a monoclinic unit cell and a *C2/c* space group. Rietveld refinement in the Materials Studio package led to the lattice parameters a = 10.140(3) Å, b = 31.233(9) Å, c = 10.122(3) Å, and β = 90.21(2) ° with the profile factors R_{wp} = 4.80 % and R_p = 3.74 %. The C_{60} molecules are orientationally ordered and located on the Wyckoff site 4e with the coordinates of its center of mass (0, 0.13823(25), 0.25). $CBrCl_2H$ is located on Wyckoff site 8f implying that the asymmetric unit must contain only half a solvent molecule with a final refined position for the central carbon atom at (0.483(2), 0.001(4), 0.708(2)). The halogen atoms of this molecule are once again disordered with occupancies of 1/2 Cl:1/2 Br,1/2 Cl:1/2 Br, 1 Cl, indicating that one site possesses 50/50 disorder, while another site is fully occupied by a chlorine atom. Such behaviour has been proposed for the monoclinic structure of a polymorph of pure $CBrCl_2H$ named "mode 1"[32]. The molecular arrangement of the motifs is shown in Fig. 7.

Based on the disorder, the $CBrCl_2H$ molecule exhibits C_s symmetry in the monoclinic solvate, whereas in the hexagonal C_{60}·2$CBrCl_2H$ solvate, it exhibits C_{3v} symmetry in the prismatic voids of the hexagonal lattice. Thus, in the monoclinic solvate intermolecular interactions between the coexisting chemical species, C_{60} and $CBrCl_2H$, would be more anisotropic than those in the hexagonal solvate. As a consequence, the hexagonal solvate should demonstrate comparatively weaker intermolecular interactions than the solvate with lower symmetry. This observation could be extended to solvates with similar halogenated structures as can be seen in Fig. 8 in which the volume of the asymmetric unit of several halogenated solvates has been plotted against the van der Waals volume of the solvent molecule for hexagonal and monoclinic or orthorhombic solvates. For the hexagonal solvates an increase in the molecular volume of the solvent gives rise to an increase in the volume of the solvate lattice, whereas for the solvates possessing a lower symmetry lattice, the solvate volume is more scattered.

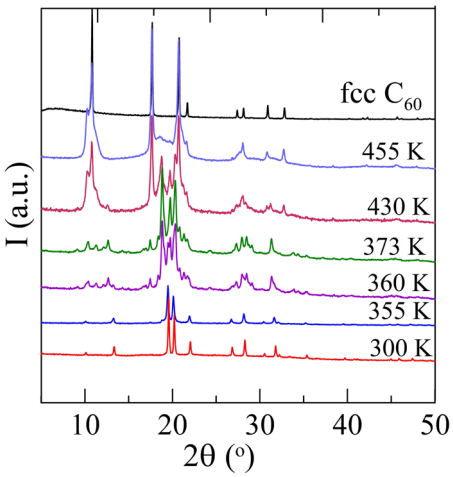

Fig. 5. X-ray diffraction patterns as a function of temperature: 300 and 355 K C_{60}·2$CBrCl_2H$; 360 K: C_{60}·2$CBrCl_2H$ + L + C_{60}·$CBrCl_2H$; 373 K: C_{60}·$CBrCl_2H$ + L; 430 K: C_{60}·$CBrCl_2H$ + L + fcc C_{60}; 455 K: L + fcc C_{60} with stacking defects. The pattern of pure fcc C_{60} is shown at the top for reference purposes.

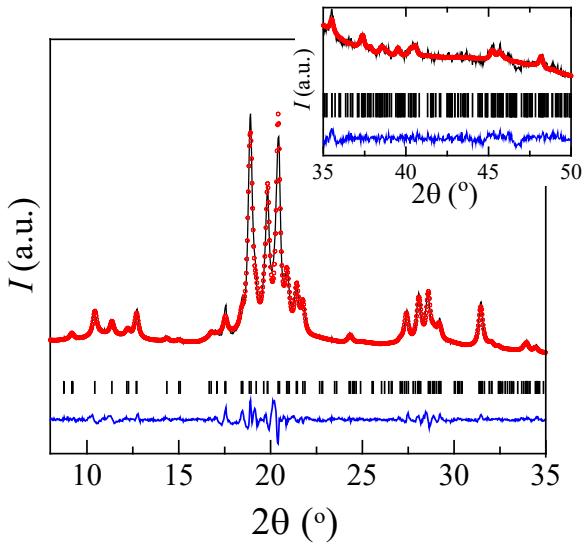

Fig. 6. Experimental (red circles) and calculated (black line) X-ray powder diffraction patterns at room temperature along with the difference profile (blue line) and Bragg reflections (vertical bars) of the monoclinic (*C2/c*) C_{60}·$CBrCl_2H$ solvate. The inset provides the data between 35 and 50° (2θ) at an increased scale.

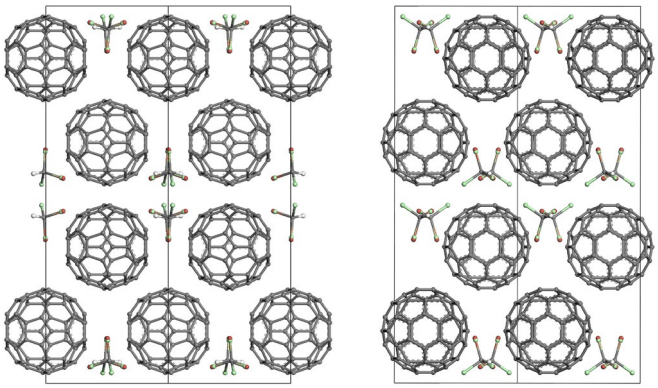

Fig. 7. The (001) plane (left panel) and the (010) plane (right panel) of the crystal structure of monoclinic (*C2/c* space group) C_{60}·$CBrCl_2H$ at room temperature. The overlap of the red (Br) and green (Cl) halogen atoms highlight the occupational disorder according to mode 1[32].

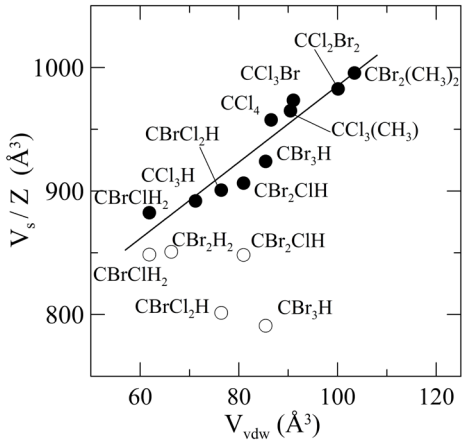

Fig. 8. Volumes of the asymmetric unit (V_s/Z) of C_{60} hexagonal (filled circles) and monoclinic or orthorhombic (open circles) solvates against the van der Waals volume of its solvent molecule.

Conclusions

The C_{60}·$2CBrCl_2H$ solvate exhibits a hexagonal structure, space group P6/mmm, as revealed by X-ray powder diffraction. The crystals are not stable when left against the air at room temperature. Both C_{60} and $CBrCl_2H$ exhibit orientational disorder. While the C_{60} molecules are isotropically disordered, for the $CBrCl_2H$ molecules the positions of the halogen atoms are distributed over 3 sites with occupancies 1/3 and 2/3 for Br and Cl atoms, respectively. This disorder exhibited by the solvent molecules occupying the prismatic voids in the hexagonal lattice corresponds to mode 2 observed in the monoclinic structure of pure $CBrCl_2H$ by Katrusiak[32].

The hexagonal solvate transforms in closed pans through a peritectic equilibrium when heated to 373 K into a lower symmetry lattice, which is monoclinic *C2/c*, while the stoichiometry changes to 1:1. In this monoclinic 1:1 solvate, C_{60} molecules exhibit orientational order, while the solvent molecule exhibits a 50/50 occupational disorder over two sites between one chlorine and one bromine atom similar to mode 1 observed in the monoclinic structure of pure $CBrCl_2H$ by Katrusiak[32].

Finally, this study shows that intermolecular interactions between the two chemical species forming the C_{60} co-crystals force the system to display a high-symmetry lattice with orientational disorder or a low-symmetry lattice with orientational order.

Supporting Information

Crystallographic information files for hexagonal C_{60}·$2CBrCl_2H$ ($CBrCl_2H$_P6mmm_sphs.cif), at room temperature, and monoclinic (C_{60}-$CHCl_2Br$-C2surC-Rietveld.cif) co-crystals, both at room temperature.

Conflict of interest

The authors declare no competing financial interests.

Acknowledgements

We thank Dr I. López (Department of Materials and Metallurgic Engineering, UPC) for his assistance with the SEM experiments. This work has been supported by the Spanish Ministry MICINN (FIS2017-82625-P) and by the Catalan government (2017SGR-42).

References

1 O. Gunnarson, Rev. Mod. Phys., 1997, **69**, 575.

`

2 M. V. Korobov, E. B. Stukalin, A. L. Mirakyan, I. S. Neretin, Y. L. Slovokhotov, A. V. Dzyabchenko, A. I. Ancharov and B. P. Tolochko, Carbon., 2003, **41**, 2743-2755.
3 R. Céolin, D. O. López, M. Barrio, J. Ll. Tamarit, P. Espeau, B. Nicolaï, H. Allouchi, and R. J. Papoular, Chem. Phys. Lett., 2004, **399**, 401-405.
4 S. Toscani, H. Allouchi, J. Ll. Tamarit, D. O. López, M. Barrio, V. Rassat, A. Agafonov, H. Szwarc and R. Céolin, Chem. Phys. Lett., 2000, **330**, 491-496.
5 M. Korobov, A. L. Mirakyan, N. V. Avramenko, G. Olofsson, A.L. Smith and R.S. Ruoff, J. Phys. Chem. B., 1999, 103, 1339-1346.
6 H. Y. He, J. Barras, J. Foulkes and J. Klinowski, J. Phys. Chem. B., 1997, **101**, 117-122.
7 M. T. Rispens, A. Meetsma, R. Rittberger, C. J. Brabec, N. S. Sariciftci and J. C. Hummelen, Chem. Comm., 2003, **17**, 2116–2118.
8 K. B. Ghiassi, M. M. Olmstead and A. L. Balch, Chem. Commun., 2013, **49**, 10721-10723.
9 L. Zheng and Y. J. Han, Phys. Chem. B., 2012, **116**, 1598–1604.
10 L. Wang, J. Phys. Chem. Solids., 2015, 84, 85–95.
11 S. Pekker, É. Kováts, G. Oszlányi, G. Bényei, G. Klupp, G. Bortel, I. Jalsovszky, E. Jakab, F. Borondics, K. Kamarás, M. Bokor, G. Kriza, K. Tompa and G. Faigel, Nat. Mater., 2005, **4**, 764–767.
12 J. Ye, M. Barrio, R. Céolin, N. Qureshi, Ph. Negrier. I. B. Rietveld and J. Ll. Tamarit, CrystEngComm, 2018, **20**, 2729-2732.
13 M. M. Olmstead, F. Jiang, and A. L. Balch, Chem. Commun., 2000, **0**, 483-484.
14 M. Barrio, D. O. López, J. Ll. Tamarit, P. Negrier and Y. Haget, J. Mater. Chem., 1995, **5**, 431-439.
15 L. C. Pardo, M. Barrio, J. Ll. Tamarit, D. O. López, J. Salud, P. Negrier and D. Mondieig, Chem. Phys. Lett., 1999, **308**, 204-210.
16 J. Salud, D. O. López, M. Barrio, J. Ll. Tamarit, H. A. J. Oonk, P. Negrier and Y. Haget, J. SOLID. STATE. CHEM., 1997, **133**, 536-544.
17 F. Michaud, M. Barrio, S. Toscani, D.O. López, J.Ll. Tamarit, V. Agafonov, H. Szwarc and R. Céolin, Phys. Rev. B., 1998, **57**, 10351.
18 M. Barrio, D. O. López, J. Ll. Tamarit, P. Espeau and R. Céolin, Chem. Mater., 2003, **15**, 288-291.
19 R. Céolin, J. Ll. Tamarit, M. Barrio, D. O. López, P. Espeau, H. Allouchi and R. J. Papoular, Carbon., 2005, **43**, 417-424.
20 R. Céolin, J. Ll. Tamarit, D. O. López, M. Barrio, V. Agafonov, H. Alluchi, F. Mussa and H. Szwarc. Chem. Phys. Lett., 1999, **314**, 21–26.
21 M. Barrio, D. O. Lopez, J. Ll. Tamarit, H. Szwarc, S. Toscani and R. Céolin, Chem. Phys. Lett., 1996, **260**, 78-81.
22 R. Céolin, J. Ll. Tamarit, M. Barrio, D.O. López, S. Toscani, H. Allouchi, V. Agafonov and H. Szwarc. Chem. Mater., 2001, **13**, 1349-1355.
23 R. Céolin, D. O. López, B. Nicolaï P. Espeau, M. Barrio, H. Allouchi and J. Ll. Tamarit, Chem. Phys., 2007, **342**, 78-84.
24 J. Ye, M. Barrio, R. Céolin, N. Qureshi, I. B. Rietveld and J. Ll. Tamarit, Chem. Phys., 2016, **477**, 39-45.
25 J. Ye, M. Barrio, Ph. Negrier, N. Qureshi, I. B. Rietveld, R. Céolin and J. Ll. Tamarit, eur. phys. j. spec. top., 2017, **226**, 857–867.
26 M. J. Hardie, R. Torrens and C. L. Raston, Chem. Commun., 2003, **0**, 1854-1855.
27 F. Michaud, M. Barrio, D. O. Lopez, J. Ll. Tamarit, V. Agafonov, S. Toscani, H. Szwarc, and R. Céolin, Chem. Mater., 2000, **12**, 3595.
28 V. V. Gritsenko, O.A. D`Yachenko, N. D. Kushch, N. G. Spitsina, E. B. Yagubskii, N. V. Avramenko and M. N. Forlova, Russ. Chem. Bull., 1994, **43**, 1183-1185.
29 A. Talyzin, and U. Jansson, J. Phys. Chem. B., 2000, **104**, 5064-5071.
30 A. O'Neil, C. Wilson, J.M. Webster, F.J. Allison, J.A.K. Howard and M. Poliakoff, Angew. Chem. Int. Ed., 2000, **41**, 3796-3799.
31 R. E. Dinnebier, O. Gunnarsson, H. Brumm, E. Koch, A. Huq, P. W. Stephens and M. Jansen, Science., 2002, 296, 109-113.
32 K. Dziubek, M. Podsiadło and A. Katrusiak, J. PHYS. CHEM. B., 2009, **113**, 13195–13201.
33 MS Modeling (Materials Studio) version 5.5, http://www.accelrys.com /mstudio/ms_modeling.
34 J. Rodriguez-Carvajal, T. Roisnel and J. Gonzales-Platas, FullProf suite (2005 version). CEA-CNRS, CEN Saclay, France: Laboratoire Léon Brillouin, 2005.
35 M. Jansen and G. Waidmann, Z. ANORG. ALLG. CHEM., 1995, 621, 14-18.
36 C. Collins, J. Foulkes, A. D. Bond and J. Klinowski, Phys. Chem. Chem. Phys., 1999, **1**, 5323-5326.
37 G. B. M. Vaughan, Y. Chabre, and D. Dubois, Europhys. Lett., 1995, **31**, 525-530.

Graphical Abstract